SAR Measurement Procedure for Multi-antenna Transmitters

Takahiro Iyama, Teruo Onishi

Research Laboratories, NTT DOCOMO, INC.
3-6 Hikari-no-oka, Yokosuka, Kanagawa 239-8536 Japan.
iyama@nttdocomo.co.jp

***Abstract*— This paper proposes and verifies a SAR measurement procedure for a multi-antenna transmitter that requires the measurement of two-dimensional electric field distributions for the number of antennas and the calculation for obtaining the three-dimensional SAR distributions for arbitrary weighting coefficients of the antennas prior to determining the average SAR. The proposed procedure is verified based on the FDTD calculation and the measurement using EO probes.**
Key words: specific absorption rate (SAR), multi-antenna, electro-optic (EO) probe, equivalent theorem, image theory.

I. INTRODUCTION

Since a multi-antenna transmitter, e.g. in Multi-Input Multi-Output (MIMO) systems, will be implemented in the user equipment (UE) of mobile communication systems in the near future [1], a Specific Absorption Rate (SAR) measurement procedure for such transmitters shall be established. Some studies focused on the SAR caused by multiple antennas from the viewpoints of the distance between the antennas and lossy objects, the spacing of the antennas, or the phase difference of the feeds [2]-[4]. Moreover, a procedure for estimating the SAR for multi-antenna transmitter was proposed in [5].

Electric field probes comprising diode-loaded dipole sensors are commonly used [6] for SAR measurement, in which it is difficult to obtain the phase of the detected electric field. The proposed procedure in [5] allows the worst-case SAR to be obtained at each point for lossy objects when the weighting coefficients for the antennas are changed. Based on the worst-case SAR, however, the averaging scheme may yield an over- or under- estimation due to extrapolation and interpolation [7]. On the other hand, some studies with respect to the electro-optic (EO) probes were conducted for SAR measurement [8], with which the amplitude and the phase of the detected electric field can be obtained.

Based on this background, we propose a SAR measurement procedure for a multi-antenna transmitter. The SAR distribution for the arbitrary weighting coefficients for the antennas can be calculated using the measured amplitude and phase of the two-dimensional electric field distribution produced by the radiation from each antenna, detected using the EO probe. Based on the SAR distribution, which can be obtained using the equivalent theorem and image theory [9], the average SAR can be calculated for the arbitrary weighting coefficients, and the maximum average SAR can be obtained for a multi-antenna transmitter.

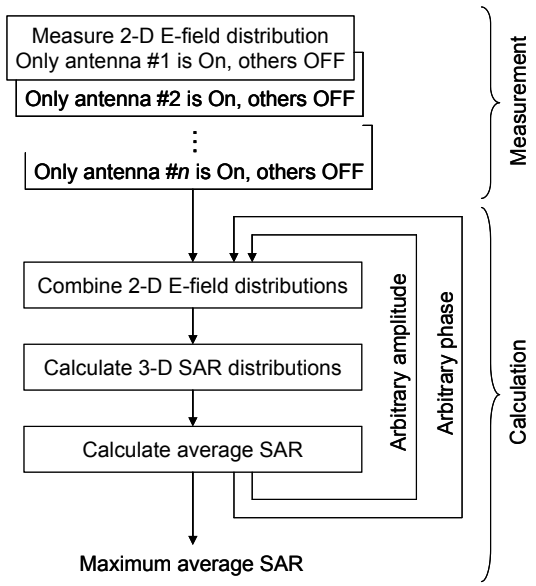

Fig. 1 Proposed procedure to determine maximum average SAR for multi-antenna transmitter

II. PROCEDURE

For the arbitrary amplitude and phase of multi antenna, the three-dimensional SAR distribution and the average SAR can be obtained as described hereafter. Figure 1 shows a flowchart of the proposed procedure for a multi-transmitter. The number of antenna is n.

1. Measure the two dimensional electric field distribution when only antenna #i is ON ($1 \le i \le n$), the others OFF.
2. Combine two-dimensional electric field distributions.
3. Calculate the three-dimensional SAR distributions based on the equivalence theorem and image theory [9].
4. Calculate the average SAR according to the procedure in [7].

The maximum average SAR can be obtained by repeating steps 2 to 4 with changing both amplitude of each antenna and

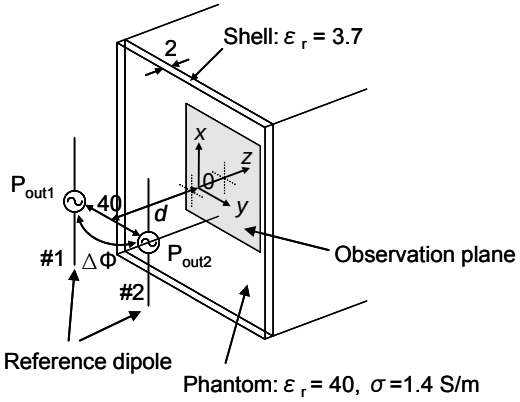

Fig. 2 Verification model

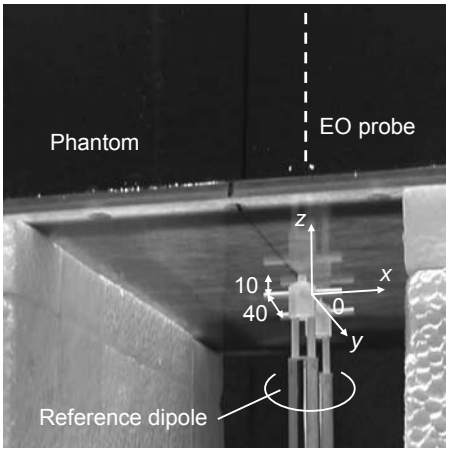

Fig. 3 Experimental configuration

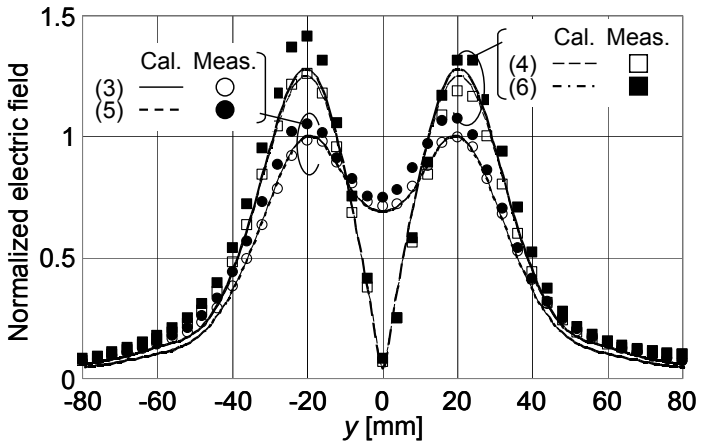

(a) Amplitude

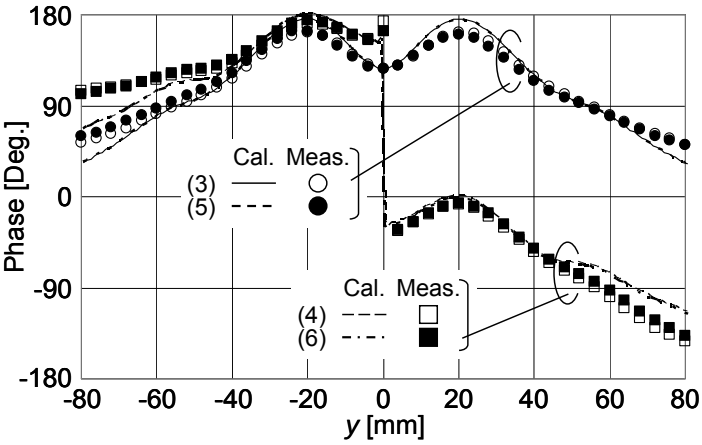

(b) Phase

Fig. 4 The *x*-component of the electric field distribution along the *y* axis while *z* = 4.5 mm in the calculation and *z* = 4 mm in the measurement

phase difference between each antenna in the ranges of the practicable weighting coefficients for the antennas.

III. Verification for Obtaining 3-D SAR Distribution

A. Configuration

The procedure to obtain the three-dimensional SAR distribution for the arbitrary weighting coefficients of the antennas is numerically and experimentally verified using two reference dipoles [4] with the separate distance of 40 mm ($0.26\lambda_0$) and a flat phantom comprising a 2 mm thick shell and tissue-equivalent liquid. The frequency is 1950 MHz. Figure 2 shows the verification model for calculation including the coordinates. P_{out1} and P_{out2} are the output power of antenna #1 and #2, respectively, and $\Delta\Phi$ is the phase difference between two antennas. The electromagnetic fields are calculated using the Finite-Difference Time-Domain (FDTD) method. The cell size is 1 mm, and a perfectly matched layer (PML) absorbing boundary condition is assumed. A reference dipole antenna is modeled that comprises a 4-mm-diameter conducting wire. The relative permittivity and the conductivity of the tissue equivalent liquid are 40 and 1.4 S/m, respectively. Figure 3 illustrates the experimental configuration corresponding to the verification model in Fig. 2. Each reference dipole antenna has the diameter of 3.6 mm. The differences in the relative permittivity and the conductivity measured using the coaxial probe were within ±5% compared to those in the calculation. The EO probe, which is located at *z* = 4 mm, is used to measure the amplitude and the phase of the electric field.

B. 2-D E-field Distribution

Figures 4(a) and 4(b) show the amplitude and phase of the *x*-component of the electric field along the *y* axis while *z* = 4.5 mm in the calculation and *z* = 4 mm in the measurement. The conditions are as follows ($P_{out1} = P_{out2}$).

(1) Ant. #1: On and Ant. #2: Off
(2) Ant. #1: Off and Ant. #2: On
(3) Combination of (1) and (2), in phase
(4) Combination of (1) and (2), out of phase
(5) Ant. #1 and Ant. #2: On, in phase (original distribution)
(6) Ant. #1 and Ant. #2: On, out of phase (original distribution)

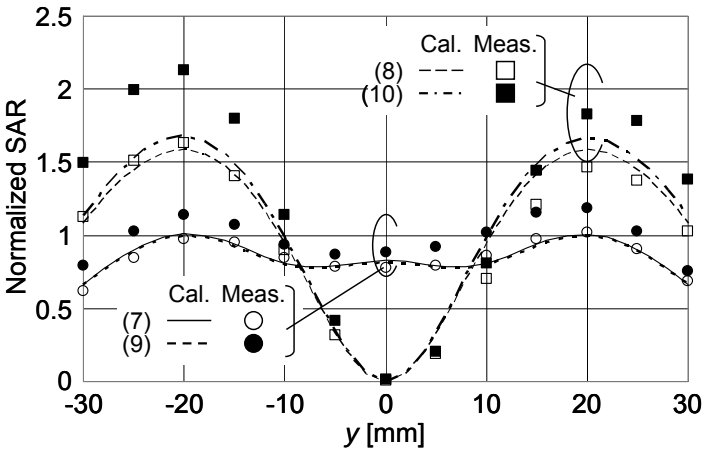

Fig. 5 SAR distribution along the *y* axis while *z* = 10.5 mm in the calculation and *z* = 10 mm in the measurement

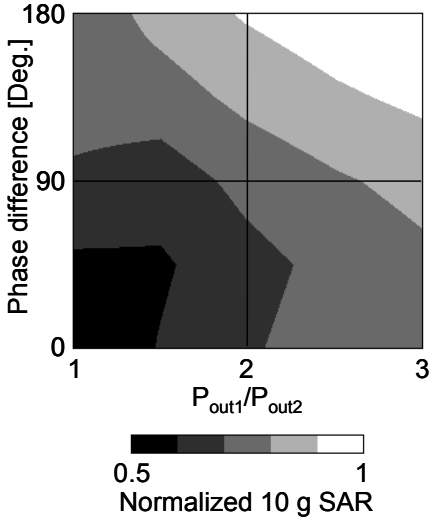

Fig. 6 10 g average SAR related to output power and phase difference of the two reference dipoles

All the lines and plots in Fig. 4(a) are normalized to the maximum electric field in case (5) above. When calculating the electric field distributions in (1) and (2), the antennas do not radiate a signal and remain in the same locations to simulate the actual measurement situation. The electric field distributions in (3) and (5) are in very good agreement both in the calculation and measurement, as well as those in (4) and (6). Therefore, the combination of electric field distributions generated by the radiation from each antenna is effective.

C. 3-D SAR Distribution

Figure 5 shows the SAR distribution obtained using the equivalence theorem and image theory [9] along the *y* axis while *z* = 10.5 mm in the calculation and *z* = 10 mm in the measurement. The conditions are given below.

(7) Based on (3), in phase
(8) Based on (4), out of phase
(9) Based on (5), in phase (original distribution)
(10) Based on (6), out of phase (original distribution)

All the lines and plots in Fig. 5 are normalized to the maximum SAR in case (9). The SAR distributions in (7) and (9) are also in good agreement based on both calculation and measurement. On the other hand, the SAR distributions in (8) and (10) exhibit some difference, especially in the measurement results. It can be considered that error in the settings of the antennas may cause such difference. However, it is indicated that the calculation of the three-dimensional SAR distribution based on the combined electric field distributions works very well.

IV. Verification for Obtaining Maximum Average SAR

In Section III, the proposed procedure is verified only in the case that the phase difference of the antennas is changed. In an actual case, however, the ratio of the output power of each antenna is expected to be parametric. The procedure to obtain the maximum average SAR is numerically verified using the configuration shown in Fig. 2. Using the three-dimensional electric field distributions in (1) and (2) described in Section III B (not *z* = 4.5 mm but for all region), the 10 g average SAR is obtained for $P_{out1}+P_{out2}$ = Constant, $1 \le P_{out1}/P_{out2} \le 3$, and the phase difference of 0 to 180˚, as shown in Fig. 6. The 10 g average SAR is normalized to the maximum one. In this case, the maximum 10 g average SAR is obtained when $P_{out1}/P_{out2} = 3$ and the phase difference is 180˚.

Under the same conditions for the antenna output power and the phase difference of the two reference dipoles, the difference of 10 g average SAR obtained from the three-dimensional electric field distributions in (1) and (2) described in Section III B compared to those from the original distribution is -2.4 %. Therefore, the process to obtain the maximum average SAR works very well.

V. Conclusion

The SAR measurement procedure for a multi-antenna transmitter was proposed and verified using a configuration comprising two reference dipole antennas and a flat phantom. It is confirmed that the procedure works very well. The features of the proposed procedure are given hereafter.

1. Only measurement of two-dimensional electric field distributions for the number of antennas is required.
2. The SAR distribution for the arbitrary weighting coefficients for the antennas can be calculated.
3. While changing the weighting coefficients of the antennas, the maximum average SAR can be numerically obtained.

If a multi-antenna transmitter has some weighting coefficients, the SAR measurement for the number of antennas is required to obtain the precise three-dimensional SAR distributions prior to obtaining the maximum average SAR. On the other hand, the proposed procedure only requires the measurement of the two-dimensional electric field distributions for the number of antennas.

It is described in [9] that the three-dimensional SAR distribution based on the two-dimensional electric field distribution using the equivalent theorem and image theory is applicable to a phantom with a curved surface, including the Specific Anthropomorphic Mannequin (SAM). Therefore, the proposed procedure can be used to measure the maximum average SAR of multi-antenna transmitters used in close proximity not only to the human body [10], which uses the flat phantom, but also to the ear [7].

REFERENCES

[1] 3GPP TR25.876, "Multi-input multi-output in UTRA," ver.7.0.0.

[2] T. Onishi and K. Ito, "Study on the characteristics of array antennas close to lossy objects," ISAP i-02, pp. 81-84, Nov. 2002.

[3] Q. Chen, Y. Komukai, and K. Sawaya, "SAR investigation of array antennas for mobile handsets," IEICE Trans. Commun., vol. E90-B, no. 6, pp. 1354-1356, June 2007.

[4] K. -C. Chim, K. C. L. Chan, and R. D. Murch, "Investigating the impact of smart antennas on SAR," IEEE Trans. Antennas Propag., vol. 52, no. 5, pp. 1370-1374, May 2004.

[5] J. Shen, R. Qiang, J. Chen, D. Jackson, M. Ayatollahi, Y. Qi, and P. Jarmuszewski, "A decomposition/superposition technique for multi-transmitter system SAR measurement," IEEE AP-S, IF417.3, July 2008.

[6] T. Schmid, O. Egger, and N. Kuster, "Automated E-field scanning system for dosimetric assessments," IEEE Trans. Microwave Theory Tech., vol. 44, no. 1, pp. 105-113, Jan. 1996.

[7] IEC 62209-1, "Procedure to determine the specific absorption rate (SAR) for hand-held devices used in close proximity to the ear (frequency range of 300 MHz to 3 GHz)," Feb. 2005.

[8] H. Togo, N. shimizu, and T. Nagatsuma, "Near-field mapping system using fiber-based electro-optic probe for specific absorption rate measurement," IEICE Trans. vol. E90-C, no. 2, pp. 436-442, Feb. 2007.

[9] K. Kiminami, T. Iyama, T. Onishi, and S. Uebayashi, "Novel specific absorption rate (SAR) estimation method based on 2-D scanned electric fields," IEEE Trans. Electromagn. Compat., vol. 50, no. 4, pp. 828-836, Nov. 2008.

[10] IEC 62209-2, "Procedure to determine the specific absorption rate (SAR) for mobile wireless communication devices used in close proximity to the human body (frequency range of 30 MHz to 6 GHz)," CDV.